European Review for Medical and Pharmacological Sciences 2021; 25: 145-153

Blocking VRK2 suppresses pulmonary adenocarcinoma progression *via* ERK1/2/AKT signal pathway by targeting miR-145-5p

Y. MU, W.-J. LIU, L.-Y. BIE, X.-Q. MU, Y.-Q. ZHAO

Department of Oncology, Affiliated Cancer Hospital of Zhengzhou University [illegible]nan Cancer Hospital, Zhengzhou, Henan Province, China

Abstract. – OBJECTIVE: The incidence of pulmonary adenocarcinoma locates first in all the malignant tumors in the world. At present, there are many diagnostic methods for pulmonary adenocarcinoma, but there are a few methods that are mature or have ideal application prospects. We aim to explore the role of VRK2 in the occurrence and development of pulmonary adenocarcinoma and its possible regulatory mechanism.

PATIENTS AND METHODS: Western blot and qRT-PCR were performed to assess the expression of VRK2. Flow cytometry, Western bl[illegible] Caspase-3 colorimetric assay Kit were u[illegible] evaluate the apoptosis level. The prolifer[illegible], migration, and invasion ability were meas[illegible] via cell cycle assay, wound healing, and tr[illegible] swell invasion assay. Luciferase assay verifie[illegible] the relationship between VR[illegible]-145-5p. The effect of FGD5-AS1 on [illegible]origen[illegible]s of glioma was detected by th[illegible]nograft[illegible] mice model.

RESULTS: VRK2 [illegible]sig[illegible]y increased in tumor tissues [illegible] cell line[illegible]s of VRK2 promoted apopt[illegible]vel and inh[illegible] the proliferation, mig[illegible] invasion i[illegible]49 cells via regulating [illegible]e ER[illegible]AKT signal pathway. Luciferase assay reporte[illegible] VRK2 could bind with mi[illegible]5-5p. The level [illegible]iR-145-5p was negat[illegible] corr[illegible]ated with t[illegible]e expression of VR[illegible]nd inv[illegible]d in VRK2 regulating tumor pro[illegible]ion[illegible]e tum[illegible] growth assay showed that t[illegible]ing of [illegible]2 inhibited tumorigen[illegible] with[illegible]activ[illegible]g ERK1/2/AKT pathway. [illegible]NCLU[illegible]nockdown of VRK2 inhibited[illegible]e deve[illegible]ent of pulmonary adenocarcin[illegible] via regulating the ERK1/2/AKT signal [illegible]geting miR-145-5p, which provid[illegible] some novel experimental basis for clinical [illegible]atment of pulmonary adenocarcinoma.

Key Words:

Pulmonary adenocarcinoma, VRK2, MiRNA, Proliferation, Metastasis.

Introduct[illegible]

Lung c[illegible]er is [illegible]unting for 27% of all malignant tumors in t[illegible]rld[1,2]. Lung cancer is split[illegible]mall cell lu[illegible]cer and non-small c[illegible]ng cancer, of which non-small cell lung c[illegible]er accounts f[illegible] about 80%. Compared with [illegible] types of l[illegible] cancer, non-small cell lung c[illegible] (NSCLC[illegible]s a relatively high degree of ma[illegible]eration, and migration[3,4]. In recent [illegible] addition to improving the therapy of tumor patients, it has become a hot spot [illegible]onary adenocarcinoma research to find [illegible]arkers that can effectively guide the early clinical diagnosis.

Vaccinia-related kinase 2 (VRK2) belongs to the vaccinia-related kinase (VRK) family of serine/threonine protein kinases[5,6]. VRK2 involved in apoptosis and tumor cell growth progression. It was reported that VRK2 plays a crucial role in schizophrenia[7]. The VRK2-Akt complex could regulate cellular proliferation and perform oncogenic activity[8]. VRK2 could promote the human breast cell line *via* activation of NFAT1 and upregulation of the level of cyclooxygenase-2[9,10]. Downregulation of VRK2 could increase the level of BAX gene, which acted as a novel meditator of apoptosis[11,12]. VRK2 also fixed KSR1-MEK1in endoplasmic reticulum forming a complex, which can have a modulatory effect on the signal mediated by MAPK[13]. However, the role of VRK2 in pulmonary adenocarcinoma has not been elucidated, which requires further investigation.

MicroRNA (miRNA) is a class of non-coding small molecule RNA, which commonly exists in prokaryotes and eukaryotes[14]. They are associated with the occurrence, development, invasion, and metastasis of various human tumors[14,15]. We predicted that VRK2 could interact with miRNA-145-5p. It was reported that

Corresponding Author: Yanqiu Zhao, MD; e-mail: 16530907585@163.com

circRNA CEP128 could sponge miR-145-5p in accelerating the development of bladder cancer by controlling SOX1[16] and Myd88/MAPK signal pathway[17]. MiR-145-5p regulates the differentiation progression of gastric cancer *via* KLF5[17]. LncRNA SNHG1 acts as a sponge of miR-145-5p promotes the development of NSCLC *via* promoting MTDH expression[18]. MiR-145-5p also inhibits EMT progression via MAP3K/JNK signaling pathway in NSCLC cells[19]. In this research, we observed that VRK2 was a target of miR-145-5p, and positively correlated with miR-145-5p, which regulates the pathways of EKR 1/2 and AKT to affect the process of pulmonary adenocarcinoma.

Patients and Methods

Clinical Samples

The tumor tissue samples and adjacent normal tissue samples were collected from 60 NSCLC patients at Affiliated Cancer Hospital of Zhengzhou University. The present study was sup[illegible]ed by the Ethics Committee of Affiliated Hospital of Zhengzhou University and als[illegible]as been carried out in accordance with the W[illegible] Medical Association Declaration of Helsinki. T[illegible] subjects had been informed th[illegible]tive. Ce[illegible] tainly, written consents we[illegible]gn[illegible]y every subject in the present study.

Cell Culture

Beas-2B, H1299, [illegible]975, SI[illegible], PG49, and A549 cell lines w[illegible]urchased fr[illegible]e Science Cell Laborator[illegible] cell lines w[illegible]cultured in PRIM 164[illegible] (Theri[illegible]sher Scientific, MA, USA) wit[illegible]% FBS (T[illegible] Fisher Scientific, MA, U[illegible] and 100 μL/mL p[illegible]cillin and streptomy[illegible] (Beyoti[illegible], Shanghai, China) and placed at [illegible] with [illegible]CO2.

Cell Transfection

[illegible]RNA ([illegible]) was produced by Ribobio Co[illegible]td. (Gua[illegible]ong, China). Si-NC (negative co[illegible]as indicated as control (si-NC). About [illegible] well were seeded in 6 well plates, [illegible]gents (20 nmol/L) were transfected into the [illegible] with Lipofectamine 2000 (Thermo Fisher Sc[illegible]ific, MA, USA) for 48 h.

SI-VRK2: 5'GCAAGGUUCUGGAUGAUAU3'; MiRNA-145-5p mimics: 5'ATCGTCCAGTTTTCCCAGG3'/5'CGCCTCCACACTCACC3'; MiRNA-NC: 5'ATTGGAACGATACA GAGAAGATT3'/5'G GAACGCTTCACGAATTTG3'. AMO-miRNA-145-5p: 5'TAG GTCAAGACTCCCCCGA 3'; A[illegible]O-NC: 5'TAGGTCAAGAGACTCCCC[illegible]

qRT-PCR

RNA isolation, reverse trans[illegible]n, and quantitative expression w[illegible] carri[illegible]ord-ing to the manufacture[illegible]nstruction[illegible] RNA was collected f[illegible] tum[illegible]or NS[illegible] cells using TRIzol [illegible]ent (I[illegible]trogen, CA, USA), DNA was [illegible]ev[illegible]t [illegible]scriptio[illegible]sing a High Capacit[illegible]NA [illegible]se Tra[illegible]ription Kit (Qiagen, S[illegible]ghai, Chi[illegible]e[illegible]me PCR program is [illegible]0 cycles. A[illegible]e program finished, [illegible]rela[illegible]RNA level[illegible] were calculated based on the C[illegible]es and normalized to the [illegible]/U6 level i[illegible]h sample. Gene level[illegible] calculated using t[illegible]e $2^{-\Delta\Delta Ct}$ method. The [illegible]er sequence[illegible] were as follows: VRK2: For-[illegible]d: 5′-AGTG[illegible]AGAAGCGCTGAGTCCT-3′; R[illegible]se: 5′-CAA[illegible]GTTCTTGAGACTCTTG-3′. GA[illegible] Fo[illegible]d: 5′-GGTCTTACTCCTTG-GAGG[illegible]TG-3′; Reverse: 5′-ACCTAAC-TACATGGTTTACATGTT-3′. miRNA-145: For-[illegible]5′-CAGTGCGTGTCGTGGAGT-3′ Re-[illegible]5′-AGGTCCAGTTTTCCCAGG-3′ U6: Forward: 5′-CTCGCTTCGGCAGCACA-3′ Reverse: 5′-AACGCTTCACGAATTTGCGT-3′.

Western Blot

Total protein was collected from tissues and cells with RIPA lysis Mix (Beyotime, Shanghai, China). Briefly, 40-60 μg protein extraction was loaded *via* SDS-PAGE and transferred onto nitrocellulose membranes (Millipore, Billerica, MA, USA), the membranes were incubated in 5% non-fat blocking solution for 3 h. Then, they were incubated with primary antibodies for 2 h at room temperature, and then, plated at 4°C for one night, After incubation with secondary antibodies, the membranes were scanned using an Odyssey, and data were analyzed with Odyssey software (LI-COR, Lincoln, NE, USA). ERK (67170-1-Ig, 1:500), AKT(10176-2-AP,1:1000), p-AKT (66444-1-Ig, 1:500) were purchased from Proteintech (Rosemont, IL, USA); p-ERK (sc-7383, 1:200) was purchased from SANTA CRUZ Biotechnology (Santa Cruz, CA, USA), VRK2 (ab58052, 1:500) were purchased from Abcam (Cambridge, UK), and GraphPad (60004-1-Ig, 1:2000) was used as an internal control.

CCK-8 Assay

Cells were cultured in 96-well cell plates and added CCK-8 buffer (MedChemExpress, Monmouth Junction, NJ, USA) at 0, 24, 48, and 72 h. 2 h later, measure 450 OD value with an MK3ELISA photometer (Thermo Fisher Scientific, Waltham, MA, USA).

Matrigel Invasion Assay

Cells in the logarithmic growth phase were adjusted to 2 × 10^5 cells/well of medium (without serum) and plated 1μg/μl Matrigel into the upper chamber. The lower chamber was added with 500 μL of the medium, and then incubate the plate at 37°C for 48 h. Then, the invading cells were visualized by the crystal violet and inverted microscope.

In Vivo Tumor Growth Assay

Nude mice were purchased from the Beijing Charles River. Stable VRK2 knockdown cell lines were constructed, A549 cells (5 × 10^6) were subcutaneously injected in the right lower limb of the nude mice. Tumor size was measured every five days. After another 15 d of injection, the tumor was removed for follow-up study. This animal study was approved by the Animal Ethical Committee of Affiliated Cancer Hospital of Zhengzhou University. Nude mice were euthanized and operated strictly in accordance with the Guidelines for the Care and Use of Laboratory Animals of the National Institutes of Health.

Cell Apoptosis Assay

The A549 cells were resuspended 5×10 cells/mL. Then, 1 mL were centrifuged, 1000 rpm, 10 min, 4°C, and the medium was throw away. The cells washed with PBS and dropped medium. The cells were resuspended and avoided light for 15 min with 5 μL Binding Buffer with 5 μL Annexin V-FITC and 10 μL PI. Flow cytometry was used to measured apoptosis rate within 1 h.

Cell Cycle Assay

A549 cells collected with 1 ml trypsin for 1 min, suspension the cell with 5 ml PBS, centrifuged at 1000 RPM for 5 min at 4°C. 10 ml PBS was used to re-washed and dropping medium, Then, the cells were fixed with 70% ethanol overnight. The next day, the cell medium was filtered with a 300-mesh sieve, centrifuged at 1000 RPM at 4°C for 5min, and the supernatant was discarded. The cells were avoided light and fixed with 1ml PI solution and stated at 4°C for 30 min. Flow cytometer was used to evaluate the cell cycle.

Luciferase Assay

HEK293T cells were co-transfected 50 mmol/L miRNA mimic or miR-NC together with VRK2-WT or VRK2-mutation. Luciferase activity was measured with Dual-Luciferase Reporter Assay Kit (Thermo Fisher Scientific, Waltham, MA, USA) on GloMax20 at 48 hr after transfection.

Immunohistochemistry (IHC)

The tumor tissue was cut into 5-μm-thick sections. The sections were dewaxed and deparaffinized in xylene and rehydrated in gradient alcohol solutions. Sections were heated in the Tris-EDTA buffer for 2 min to extract antigen. Samples were incubated with primary antibodies for ki-67 (27309-1-AP, 1:100), VEGF (19003-1-AP, 1:100), p-ERK (sc-7383, 1:20), p-AKT (66444-1-Ig, 1:50), cleaved-caspase3 (ab32042, 1:100, Abcam, Cambridge, UK) and HRP-labeled streptavidin (A0303, 1:200, Beyotime, Shanghai, China) secondary antibodies. Sections were avoided light with hematoxylin dehydrated and secured. Photos were taken with an Olympus camera.

Statistical Analysis

All values are expressed as the mean ± SEM. Statistical significances were measured by Student's *t*-test and ANOVA. A two-tailed value of $p < 0.05$ was indicated as a statistically significant difference. Data statistics were used the GraphPad 7.0 (La Jolla, CA, USA).

Results

VRK2 Was an Upregulation in Pulmonary Adenocarcinoma Tissue and Cells

To detect the role of VRK2 in pulmonary adenocarcinoma, we collected tumor and para-cancer tissue from 60 pulmonary adenocarcinoma patients. By performing qRT-PCR assays, we found VRK2 was an upregulation in tumor tissue comparing with normal tissues (Figure 1A). We also detected the level of VRK2 in different human pulmonary adenocarcinoma cell lines (H1299, H1975, SPC-A-1, PG49, and A549); the Beas-2B cell line was indicated as control. The

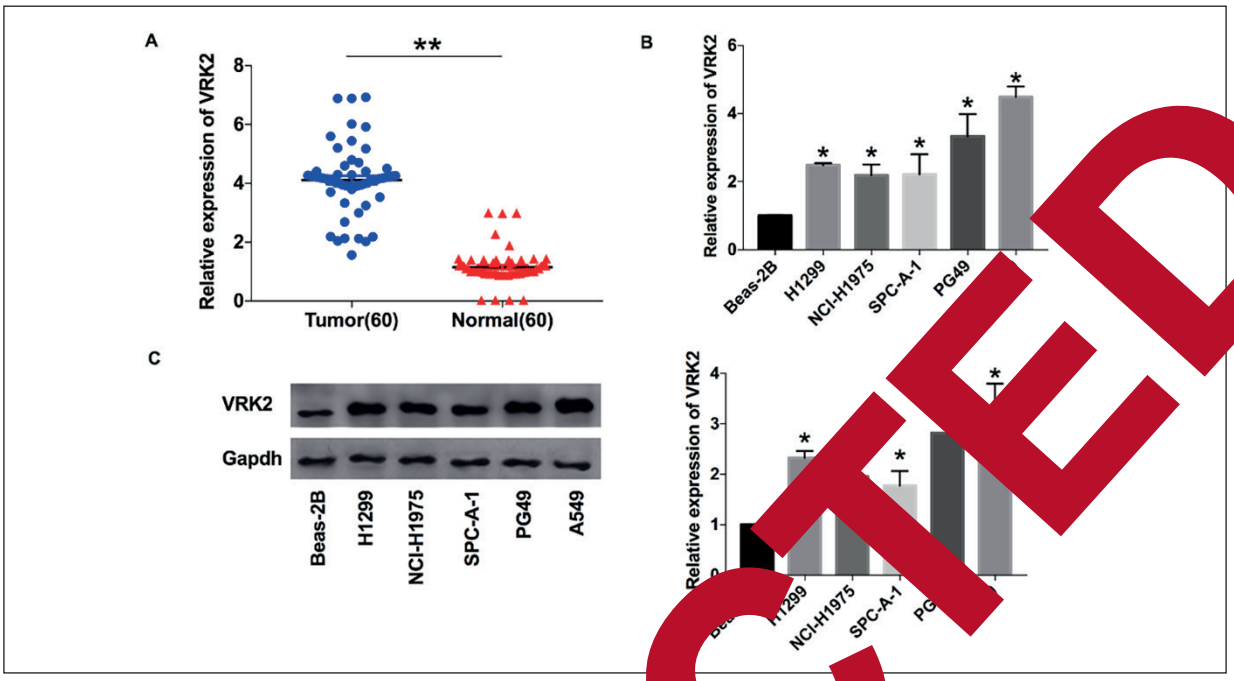

Figure 1. VRK2 expression levels in pulmonary adenocarcinom[illegible]ues and cell[illegible]s. **A,** RT-PCR detected the mRNA level of VRK2. n=60, **p <0.01. **B,** The mRNA level of VRK2 in pu[illegible]y adeno[illegible]noma cell lines (H1299, NCI-H1975, SPC-A-1, PG49, A549), Beas-2B cell line was identified as a contro[illegible]05. **C,** The protein level of VRK2 in pulmonary adenocarcinoma cell lines. n=6, *p <0.0[illegible]

results showed that VRK2 was increased in[illegible] ter 72 h, si-VRK2 significantly inhibited cell proliferation (Figure 3A). To further link VRK2 expression to cell invasion, we applied the chamber-transwell invasion assay. The results showed that VRK2 downregulation could block cell invasion in cells (Figure.3B). Figure.3C showed that si-VRK2 inhibited A549 migration at 24 h and 48 h. Downregulation of VRK2 inhibited the activation of AKT and ERK1/2. (Figure 3D).

Knockdown of VRK2 [illegible]mote[illegible] Apoptosis of A549

Next, we would [illegible]y the [illegible]n of VRK2 in pulmonary ad[illegible]arcinoma. [illegible]nstructed siRNA to kno[illegible]e expressio[illegible] VRK2. Si-VRK2/si-N[illegible] were t[illegible]cted into A549 cells; then, flow[illegible]tometry pe[illegible]d that the apoptosis r[illegible]as significantly [illegible]eased in the si-VRK[illegible]roup c[illegible]pare with si-NC (Figure 2A). Th[illegible]e dis[illegible]ered significantly increased G0/G1 ce[illegible]ecrease[illegible] cells after downregula-[illegible] VR[illegible]igure[illegible]. Furthermore, we detect-[illegible] caspa[illegible]ty and apoptosis-associated pro[illegible], cleave[illegible]ARP, Bcl-2, cleaved-caspase3, cl[illegible]aspase8, cleaved-caspase9 (Figure [illegible]D), [illegible]esults showed that knockdown of [illegible]RK2 could facilitate apoptosis of A549 cell.

K[illegible]kdown of VRK2 Prevents Proliferation and Metastasis of A549

Then CCK8 assay was carried out to evaluate the function of VRK2 on NSCLC cell prolifer-

VRK2 Could Interact With MiR-145-5p

Bioinformatics sites showed that VRK2 was negatively correlated with miRNA-145-5p and that miRNA-145-5p could bind with the 3 'UTR region of VRK2 (Figure 4A&B). To verify the forecast, we created miR-145-5p mimics/miR-NC and performed Luciferase assay; the report confirmed the link between VRK2 and miRNA-145-5p (Figure 4C). We transfected si-VRK2/si-NC, miR-145-5p mimics/AMO-145-5p/miR-NC into A549 cells to measure the expression of miR-145-5p and VRK2, there was a negative correlation between VRK2 and miRNA (Figure 4D&E). Meanwhile, AMO-145-5p could block the inactivation of AKT and ERK1/2 induced by si-VRK2 (Figure 4F). In summary, interacting with miR-145-5p, VRK2 participated in the proliferation

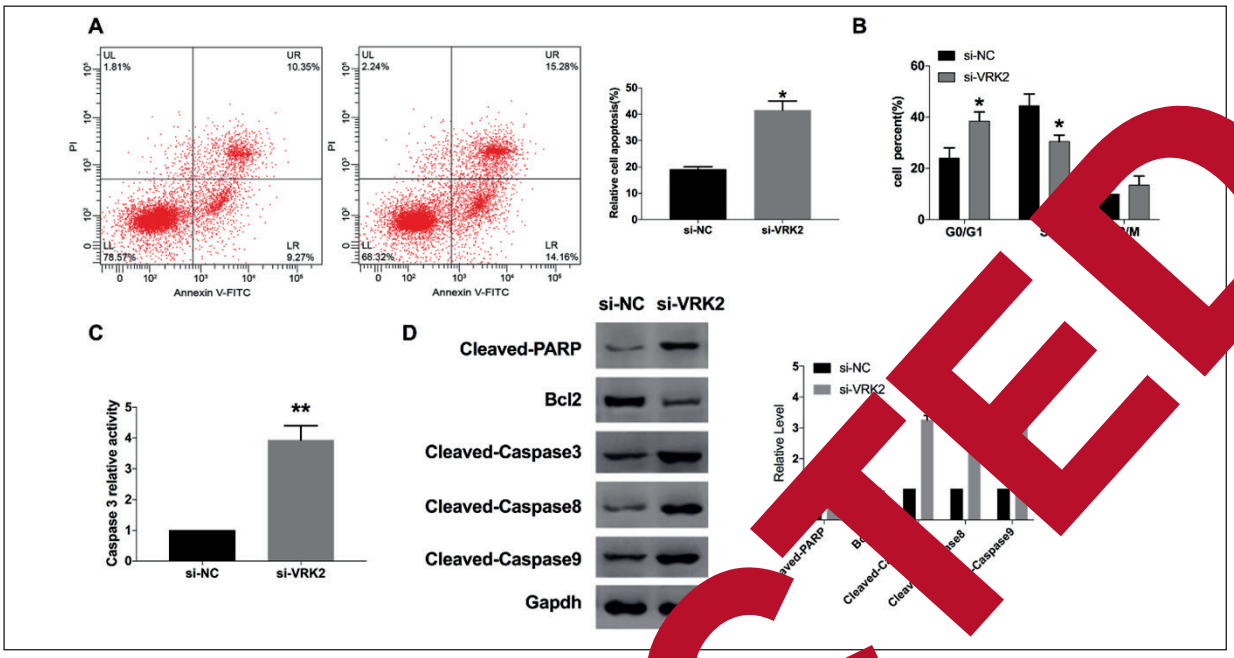

Figure 2. Knockdown of VRK2 promotes apoptosis in A549 cel . The apoptosi e was measured by flow cytometry. n=6, **p* <0.05. **B,** The effect of VRK2 on cell cycle. n=5, **p* < C, Si-VRK2 ced Caspase-3 activation in A549 cells. n=6, **p* <0.05. **D,** The protein level of apoptosis-associated pr (Cleaved- P, Bcl2, Cleaved Caspase3, Cleaved Caspase8, Cleaved Caspase9) was detected in A549 after si-VRK2/si-N =8, **p* <0.05.

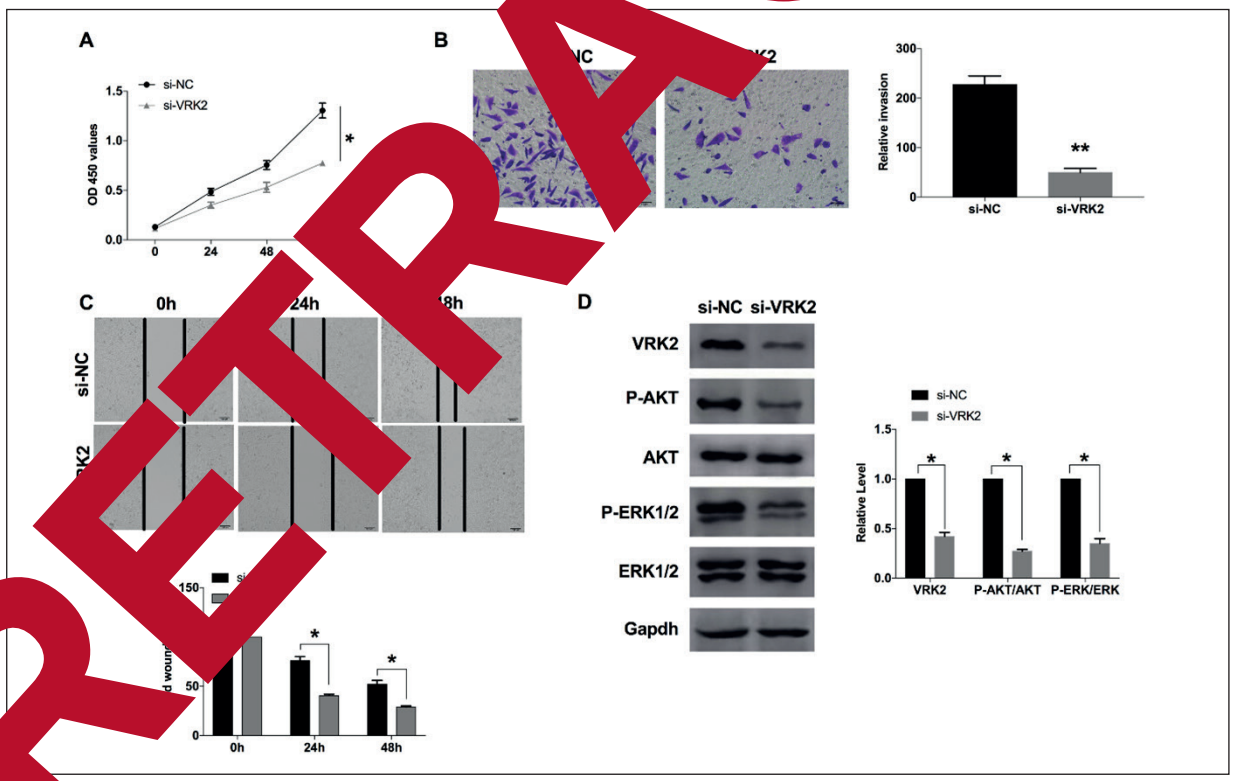

Figure 3. Knockdown of VRK2 inhibits proliferation and metastasis via AKT/ERK1/2 signal pathway in A549 cells. **A,** CCK assay was performed to detect the proliferation ability. n=4, **p* <0.05. **B,** Cell invasion ability was detected in A549 after si-VRK2/si-NC transfection (magnification×100). n=6, **p*<0.05. **C,** Representative images (left) and histogram (right) from wound-healing assays using A549 cells. n=4, **p* <0.05. **D,** The protein level of VRK2, AKT, p-AKT, ERK1/2, p-ERK1/2 were identified by Western blot. n=6, **p*<0.05.

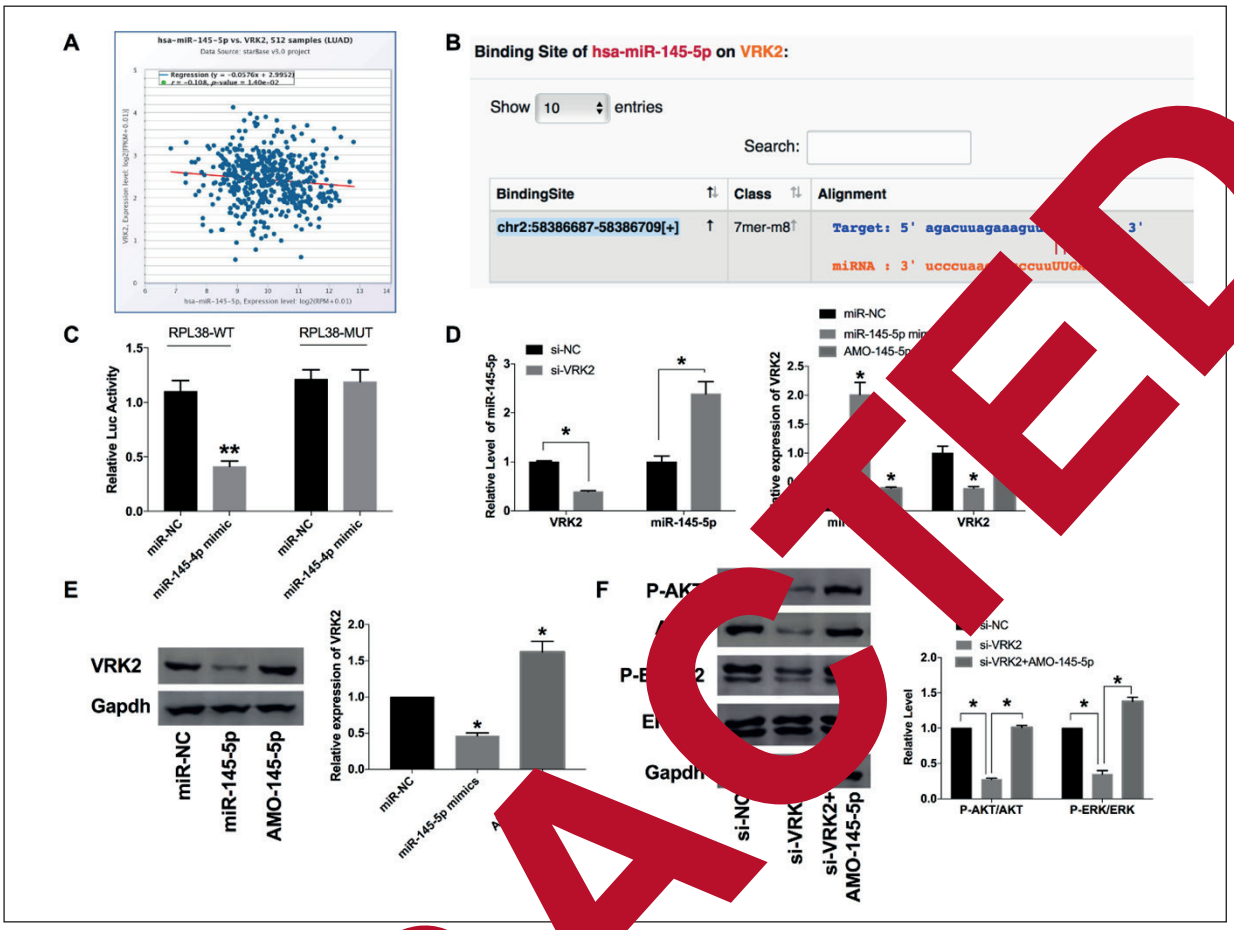

Figure 4. MiR-145-5p banding v[illegible]egulates [illegible]ERK1/2 signal pathway. **A,** Bioinformatics predicted the relationship between miR-145-5p[illegible]VRK2. [illegible]bioinforma[illegible]predicted the binding sequence of miR-145-5p to VRK2. **C,** Luciferase assay reported miR[illegible]p interac[illegible]with VRK2. n=4, *$p < 0.05$. **D, E,** Regulatory effects between miR-145-5p and VRK2 was detected by R[illegible] n=8. [illegible]protein level of AKT, p-AKT, ERK1/2, p-ERK1/2 was detected by Western blot. n=6, *p <[illegible]5.

and metastasis[illegible]cells *via* re[illegible]ting the ERK1/2 and A[illegible]T sign[illegible]hway.

Knock[illegible]vn of VRK2 Pr[illegible]its Tumor Gro[illegible] In Vi[illegible]

[illegible]urthe[illegible]nfirmation, we constructed a stable [illegible]pressio[illegible]VRK2 A549 cell (si-[illegible]K2-A[illegible]the [illegible]al level of VRK2 A549 [illegible]s a [illegible](si-NC-A549). Two groups of [illegible]49 cells [illegible]re randomly and subcutaneou[illegible]ected in the right lower limb of the [illegible]tumor size was measured every [illegible]e days. Si-VRK2-A549 injection group significantly reduced tumor volume and weight (Figure 5A-C). The tumor tissues of the si-VRK2-A549 injection group showed a higher level of miR-145-5p and a lower level of VRK2 compared with si-NC-A549 (Figure 5D&E), the phosphorylation of AKT and ERK1/2 were also decreased in si-VRK2-A549 injection mice (Figure 5F). The tumor tissue was sectioned for immunohistochemical staining (Figure 5G). The Ki-67 staining performed that VRK2 knockdown significantly inhibited the proliferation of tumo, which got similar results *in vitro*. Si-VRK2-A549 decreased the level of VEGF, p-ERK, and p-AKT, accompanied by increased expression of cleaved-Caspase3.

Discussion

Until now, the commonly used tumor markers such as carcinoembryonic antigen (CEA) have a specific value in the diagnosis of the tumor; their sensitivity and specificity are not high enough[20,21].

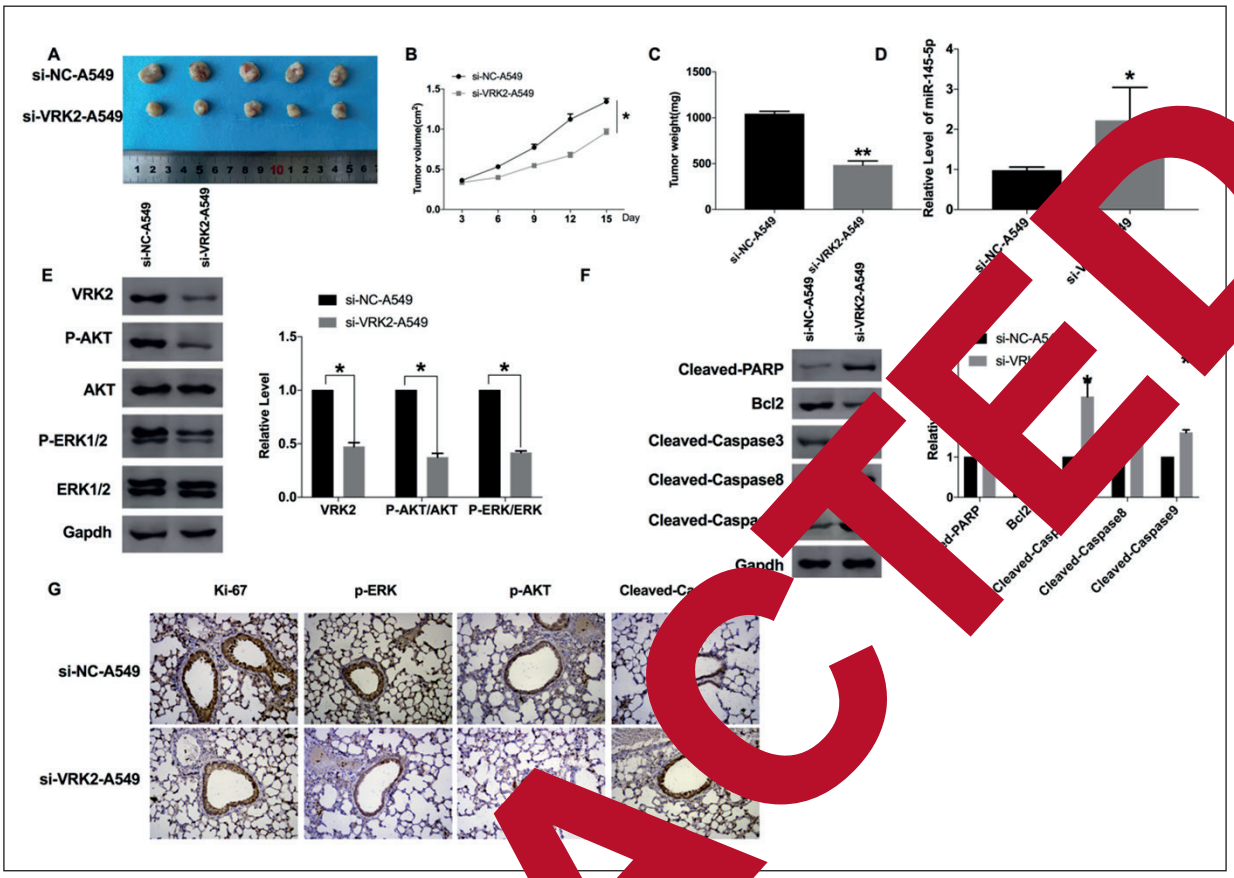

Figure 5. VRK2 regulates tumorigenesis *in vivo*. **A,** [illegible] VRK2 knockdown on the size of A549 xenograft tumors in nude mice. **B, C,** The significantly small[illegible]rage tumor [illegible]e and weights of the si-VRK2-A549 group are compared to the si-NC-A549 group. **D,** The mRNA le[illegible]145-5p in [illegible]r tissue. n=6, *$p < 0.05$. **E,** The protein level of VRK2, AKT, p-AKT, ERK1/2, p-ERK1/2 were d[illegible]ed by [illegible]tern blot. [illegible]*$p<0.05$. **F,** The protein level of apoptosis-associated protein (Cleaved-PARP, Bcl2, Cleaved C[illegible]se3, Clea[illegible]Caspase8, [illegible]eaved Caspase9) were detected in tumor tissue. n=8, *$p < 0.05$. **G,** Representative images (Ma[illegible]tion×2[illegible]taining of ki67, p-ERK, p-AKT, and Cleaved-caspase3.

The early diagno[illegible] pulmonary [illegible]ocarcinoma is severe, t[illegible]p[illegible]sis of patie[illegible]s weak, the late survi[illegible] perio[illegible]short, especially the pulmonar[illegible]denocarcinol[illegible]he incidence rate is lowe[illegible]an other types o[illegible]monary adenocarci[illegible]a, the [illegible]t age is smaller, and the lump gr[illegible]s slo[illegible]o it is more accessible to misdiagnos[illegible]rough t[illegible]bioinformatics analysis [illegible]ulmo[illegible]aden[illegible]inoma, a large number of s[illegible] have[illegible]ported on the development, me[illegible]asis, dr[illegible]esistance, and prognostic mole[illegible]rkers of pulmonary adenocarcinoma[24]. [illegible]y d[illegible]s of pulmonary adenocarcinoma is [illegible] essential factor in improving the prognosis and [illegible]al survival rate of pulmonary adenocarcinom[illegible]ients. But the diagnosis and treatment are not satisfactory[25]. Therefore, we need to explore further the mechanism of pulmonary adenocarcinoma, which could provide a new index for early diagnosis and therapy of pulmonary adenocarcinoma.

In previous studies, VRK2 was an abnormal expression in psychiatric disorders and epilepsies. In an earlier study, VRK2 was identified as a potential mental and neurological disorder, but few studs on tumors, especially in pulmonary adenocarcinoma. It was reported that VRK2 could regulate the hypoxia stress response induced by TAK1[26]. VRK2 participated in breast cancer via modulating the FBXW2-MSX2-SOX2 axis[27]. VRK1 and VRK2 were both described as an indicator of rectal adenocarcinoma response to neoadjuvant chemoradiation therapy[28]. Some shortcomings of this study are that appropriate VRK2 specific inhibitors were not used to inhibit its activity; we choose siRNA to inhibit VRK2, which may have differential results.

In our study, after quantitative detection of VRK2 level in pulmonary adenocarcinoma patients, it was

found that VRK2 expression in pulmonary adenocarcinoma tissues was significantly higher than adjacent tissues, the similar results were performed in pulmonary adenocarcinoma cell lines. Knockdown of VRK2 could promote apoptosis and press proliferation, metastasis of A549 cells. Further results showed that miR-145-5p could bind with VRK2 involved in pulmonary adenocarcinoma progression via regulating AKT/ERK1/2 signal pathway.

In recent years, the research on the function of miRNA has become one of the breakthroughs in life science, especially in the mechanism of occurrence and development of malignant tumors. MiRNA is a kind of non-coding small molecule RNA, which is widely involved in the regulation of life activities. The results show that most of the genes in human and other mammals are regulated by miRNA, and each miRNA can regulate hundreds of target genes[29,30]. With the deepening of the study of miRNA, it has been reported that the expression of miRNA has significant tissue specificity, and its expression profile analysis can be used to identify the source of tumor, and has higher accuracy than the classification m d of mRNA expression profile, and can reflect the level of gene function. Some s es have also shown that changes in the expres level of miRNA can cause changes in a se of oncogenes and tumor supp enes, a then provide an effective way tumo treatment by specifically i biting activity of carcinogenic miRN e dev f pulmonary adenocar on mplex p cess involving ma actors, and genes, involving many s[31,32]. Usin RNA microarray to an differentia pressed miRNA, in pulmona denocarcinoma and paracanc s tissues is ful to systematically s the interaction ween genes and com mole mechanisms in the develop of t nalignant tumor, and provide reliab or the ention, diagnosis and tmen ulm y adenocarcinoma.

Conclusions

For the first, we established the correlation ween VRK2 and miR-145-5p and explored the ro d underlying mechanism of VRK2 in pulmonary adenocarcinoma. Although the research is still insufficient, it also can provide a specific theoretical basis for clinical research.

Conflict of Interest

The Authors declare that they have no conflict of interests.

Funding

The authors received no funding for this w

Referenc

1) Rami-Porta R, Call S oms C hiols C, chez M, Travis WD mer I cancer staging: a concise upda r P J 2018 1.
2) Roman M, Ba ar I, Nadal olfo C, Vicent S,Gi o I KRAS gen on-small cell lung clinical pers n the treatment o et. Mol Canc 18; 17: 33.
3) Tan X, anerje ham EA, Rutaganira FUN, Basu K, Bota-Rab as N, Guo HF, Grzesko-, Liu X, Yu J, Peng DH, Rodriguez , Zhang J, Zheng V, ose DY, Solis LM, Mino B, Raso MG, Behrens C, Wistuba, II, Scott KL, Smith M uyen K, Lam G, Choong I, Magumdar A, H , Gibbons DL, Brown PH, Rus- WK, Sho K, Creighton CJ, Glenn JS, Kurie is a therapeutic target in chrom amplified lung adenocarcinoma. Sci Transl Med 2020; 12: eaax3772.
4) Ferrara R, Auger N, Auclin E, Besse B. Clinical anslational implications of RET rearrangements in non-small cell lung cancer. J Thorac Oncol 2018; 13: 27-45.
5) Li M, Yue W. VRK2, a candidate gene for psychiatric and neurological disorders. Mol Neuropsychiatry 2018; 4: 119-133.
6) Tesli M, Wirgenes KV, Hughes T, Bettella F, Athanasiu L, Hoseth ES, Nerhus M, Lagerberg TV, Steen NE, Agartz I, Melle I, Dieset I, Djurovic S, Andreassen OA. VRK2 gene expression in schizophrenia, bipolar disorder and healthy controls. Br J Psychiatry 2016; 209: 114-120.
7) Lee J, Lee S, Ryu YJ, Lee D, Kim S, Seo JY, Oh E, Paek SH, Kim SU, Ha CM, Choi SY, Kim KT. Vaccinia-related kinase 2 plays a critical role in microglia-mediated synapse elimination during neurodevelopment. Glia 2019; 67: 1667-1679.
8) Hirata N, Suizu F, Matsuda-Lennikov M, Tanaka T, Edamura T, Ishigaki S, Donia T, Lithanatudom P, Obuse C, Iwanaga T, Noguchi M. Functional characterization of lysosomal interaction of Akt with VRK2. Oncogene 2018; 37: 5367-5386.
9) Vazquez-Cedeira M, Lazo PA. Human VRK2 (vaccinia-related kinase 2) modulates tumor cell invasion by hyperactivation of NFAT1 and expression of cyclooxygenase-2. J Biol Chem 2012; 287: 42739-42750.
10) Fernandez IF, Blanco S, Lozano J,Lazo PA VRK2 inhibits mitogen-activated protein kinase signaling and inversely correlates with ErbB2 in human breast cancer. Mol Cell Biol 2010; 30: 4687-4697.

11) Monsalve DM, Merced T, Fernandez IF, Blanco S, Vazquez-Cedeira M, Lazo PA Human VRK2 modulates apoptosis by interaction with Bcl-xL and regulation of BAX gene expression. Cell Death Dis 2013; 4: e513.

12) Li LY, Liu MY, Shih HM, Tsai CH,Chen JY Human cellular protein VRK2 interacts specifically with Epstein-Barr virus BHRF1, a homologue of Bcl-2, and enhances cell survival. J Gen Virol 2006; 87: 2869-2878.

13) Fernandez IF, Perez-Rivas LG, Blanco S, Castillo-Dominguez AA, Lozano J, Lazo PA. VRK2 anchors KSR1-MEK1 to endoplasmic reticulum forming a macromolecular complex that compartmentalizes MAPK signaling. Cell Mol Life Sci 2012; 69: 3881-3893.

14) Rupaimoole R, Calin GA, Lopez-Berestein G, Sood AK. MiRNA deregulation in cancer cells and the tumor microenvironment. Cancer Discov 2016; 6: 235-246.

15) Kong YW, Ferland-McCollough D, Jackson TJ, Bushell M. MicroRNAs in cancer management. Lancet Oncol 2012; 13: e249-258.

16) Wu Z, Huang W, Wang X, Wang T, Chen Y, Chen B, Liu R, Bai P, Xing J. Circular RNA CEP128 acts as a sponge of miR-145-5p in promoting the bladder cancer progression via regulating SOX11. Mol Med 2018; 24: 40.

17) Sun M, Zhao W, Chen Z, Li M, Li S, Wu [illegible] Circular RNA CEP128 promotes bladder [illegible] progression by regulating Mir-145-5p/Myd[illegible]a MAPK signaling pathway. Int J Cancer 2019; 2170-2181.

18) Lu Q, Shan S, Li Y, Zhu D, Jin [illegible] Long non coding RNA SNHG1 promot[illegible] cell lung cancer progression by [illegible]gulating [illegible]TDH via sponging miR-145-5p. [illegible]B J 20[illegible]: 3957-3967.

19) Chang Y, Yan W[illegible]C, Li [illegible]ng J,Wang M miR-145-5p inhi[illegible]epithelial-[illegible]chymal transition via the [illegible]ignaling path[illegible] targeting MAP3K1 in [illegible]cell lung can[illegible]cells. Oncol Lett 2[illegible]14: 6[illegible]28.

20) Chen [illegible]heng R, Bac[illegible], Zhang S, Zeng H, Bra[illegible]emal A, Yu XQ,H[illegible]ancer statistics in C[illegible]2015.[illegible]A Cancer J C[illegible]2016; 66: 115-132.

21) [illegible]n H, Li[illegible]ien J, Feng X, Lyu Z, Wei L, Li X, [illegible]g Z, Zo[illegible] Zhang Y, Li J, Zhang K, C[illegible]ai M, [illegible] Group of cancer screening p[illegible]n in [illegible]C participation and yield of [illegible]popu[illegible]d colorectal cancer screening [illegible]gramm[illegible]nina. Gut 2019; 68: 1450-1457.

22) [illegible]g K, Liu CC, Mao AY, Shi JF, Dong P, Huang [illegible]B, Liu GX, Liao XZ, Bai YN, Sun XJ, Ren JS, Yang L, Wei DH, Song BB, Lei HK, Liu YQ, Zhang YZ, Ren SY, Zhou JY, Wang JL, Gong [illegible]Y, Yu LZ, Liu YY, Zhu L, Guo LW, Wang YQ, He [illegible], Lou PA, Cai B, Sun XH, Wu SL, Qi X, Zhang [illegible]K, Li N, Chen WQ, Qiu WQ, Dai M. [Analysis on the demand, access and related factors of cancer prevention and treatment knowledge among urban residents in China from 2015 to 2017]. Zhonghua Yu Fang Yi Xue Za Zhi 2020; 54: 84-91.

23) Leng A, Jing J, Nicholas S, Wang J. Ca[illegible] health expenditure of cancer patient[illegible] of-life: a retrospective observation[illegible]udy in China. BMC Palliat Care 2019; 18:[illegible]

24) Ruiz-Cordero R,Devine WP. Ta[illegible] therapy and checkpoint immunoth[illegible]py in [illegible]ancer. Surg Pathol Clin 2020; 1[illegible]33.

25) Inamura K. Clinicop[illegible]ological [illegible]characte[illegible] and mutations drivi[illegible]evelop[illegible]of early [illegible]g adenocarcinoma: [illegible]initi[illegible] and [illegible]ogression. Int J Mol [illegible]20[illegible]

26) Blanco S, S[illegible]C, Lazo [illegible]acci[illegible]lated kinase 2 m[illegible]es the stress[illegible]to hypoxia mediate[illegible]. Mol Cell B[illegible]07; 27: 7273-7283.

27) Yin Y, Xie CM, Li[illegible]n M, Chen G, Schiff R, [illegible], Sun Y. The[illegible]W2-MSX2-SOX2 axis [illegible]gulates stem cell prop[illegible]y and drug resistance of cancer cells. Proc Natl Acad Sci U S A 2019; 116: 20528-2[illegible]8.

2[illegible]Del Puerto-N[illegible]lo L, Marin-Arango JP, Fernan[illegible]z-Acenero[illegible]Arroyo-Manzano D, Martinez-Us[illegible]R[illegible]Palacios A, Rodriguez-Remirez M, Ce[illegible]omez Del Pulgar T, Cruz-Ramos M, Carames C, Lopez-Botet B, Garcia-Foncillas J. Predictive value of vrk 1 and 2 for rectal adenoma response to neoadjuvant chemoradiatie[illegible]therapy: a retrospective observational cohort study. BMC Cancer 2016; 16: 519.

29) Yu N, Yong S, Kim H, Choi Y, Jung Y, Kim D, Seo J, Lee Y, Baek D, Lee J, Lee S, Lee J, Kim J, Kim J, Lee S. Identification of tumor suppressor miRNAs by integrative miRNA and mRNA sequencing of matched tumor-normal samples in lung adenocarcinoma. Mol Oncol 2019; 13: 1356-1368.

30) Wei S, Zhang Z, Fu S, Xie J, Liu X, Xu Y, Zhao J, Xiong W. Hsa-miR-623 suppresses tumor progression in human lung adenocarcinoma. Cell Death Dis 2016; 7: e2388.

31) Molina-Pinelo S, Pastor M, Suarez R, Romero-Romero B, González De la Peña M, Salinas A, García-Carbonero R, De Miguel M, Rodríguez-Panadero F, Carnero A, Paz-Ares L. MicroRNA clusters: dysregulation in lung adenocarcinoma and COPD. Eur Respir J 2014; 43: 1740-1749.

32) Robles A, Arai E, Mathé E, Okayama H, Schetter A, Brown D, Petersen D, Bowman E, Noro R, Welsh J, Edelman D, Stevenson H, Wang Y, Tsuchiya N, Kohno T, Skaug V, Mollerup S, Haugen A, Meltzer P, Yokota J, Kanai Y, Harris C. An integrated prognostic classifier for stage i lung adenocarcinoma based on mRNA, microRNA, and DNA methylation biomarkers. J Thorac Oncol 2015; 10: 1037-1048.